THE JOURNAL OF PHYSICAL CHEMISTRY Letters

Letter

pubs.acs.org/JPCL

Femtosecond $M_{2,3}$-Edge Spectroscopy of Transition-Metal Oxides: Photoinduced Oxidation State Change in α-Fe_2O_3

Josh Vura-Weis,[†,◆] Chang-Ming Jiang,[†] Chong Liu,[†] Hanwei Gao,[†] J. Matthew Lucas,[§] Frank M. F. de Groot,[▽] Peidong Yang,[†,‡,∥] A. Paul Alivisatos,[∥] and Stephen R. Leone*[,†,‡,#]

[†]Department of Chemistry, [‡]Department of Physics, [§]Department of Mechanical Engineering, and [⊥]Department of Materials Science and Engineering, University of California, Berkeley, California 94720, United States

[#]Chemical Sciences Division and [∥]Materials Sciences Division, Lawrence Berkeley National Laboratory, Berkeley, California 94720, United States

[▽]Debye Institute for Nanomaterials Science, Utrecht University, Universiteitsweg 99, 3584 CG Utrecht, The Netherlands

Supporting Information

ABSTRACT: Oxidation-state-specific dynamics at the Fe $M_{2,3}$-edge are measured on the sub-100 fs time scale using tabletop high-harmonic extreme ultraviolet spectroscopy. Transient absorption spectroscopy of α-Fe_2O_3 thin films after 400 nm excitation reveals distinct changes in the shape and position of the 3p → valence absorption peak at ∼57 eV due to a ligand-to-metal charge transfer from O to Fe. Semiempirical ligand field multiplet calculations of the spectra of the initial Fe^{3+} and photoinduced Fe^{2+} state confirm this assignment and exclude the alternative d−d excitation. The Fe^{2+} state decays to a long-lived trap state in 240 fs. This work establishes the ability of time-resolved extreme ultraviolet spectroscopy to measure ultrafast charge-transfer processes in condensed-phase systems.

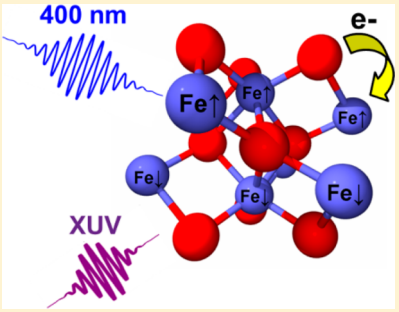

SECTION: Spectroscopy, Photochemistry, and Excited States

Time resolved X-ray absorption spectroscopy is a powerful tool for probing the electronic structure of short-lived states because of the element, oxidation state, and spin state specificity of core-to-valence transitions. With the advent of third-generation synchrotrons and free-electron lasers, photoinduced nuclear and electronic dynamics of transition-metal complexes have been studied on picosecond to femtosecond time scales.[1,2] First-row transition metals are generally probed at the K- and $L_{2,3}$-edges, corresponding to 1s → 3d and 2p → 3d transitions. There is far less work on the $M_{2,3}$-edge, or 3p → 3d transition, due to the rarity of sources in the extreme ultraviolet (XUV) spectral region from 40 to 100 eV and the need for high-vacuum sample environments. However, time-resolved spectroscopy at this edge is attractive for three reasons. First, the large overlap between the 3p and 3d wave functions leads to an absorption cross section that is 10 times larger than the $L_{2,3}$-edge and 1000 times larger than the K-edge. For solid-state samples such as transition-metal oxides, the optical and XUV cross sections are of the same order of magnitude, with similar penetration depths for pump and probe beams. Second, the Coulomb and exchange coupling between the 3d electrons and the 3p core−hole produces a multiplet peak shape that is indicative of the ligand field, oxidation state, and spin state of the metal.[3] Finally, recent advances in high-harmonic generation (HHG)[4] enable transient absorption spectroscopy to be reliably performed in the XUV using a tabletop laser-based source, with a photon flux that is 2 orders of magnitude higher than femtosecond "slicing" beamlines and the time resolution from the femtosecond[5,6] to attosecond[7,8] regimes. Tabletop XUV spectroscopy has recently been used to measure gas-phase dynamics of small molecules,[5,8] dielectric switching in Si,[7] and element-specific spin dynamics in NiFe alloys and multilayers.[9,10]

In this work, it is shown that $M_{2,3}$-edge transient absorption spectroscopy can be used to measure photoinduced oxidation state changes in a condensed-phase sample, α-Fe_2O_3 (hematite), which is a stable, earth-abundant semiconductor that is the subject of intense study due to its potential as a photocatalyst for water splitting.[11] The efficiency is hampered by low electron mobility and rapid trapping of the initial photoexcited state. The nature of this initial state is a subject of continued debate due to the complex electronic structure of this material.[12−18] Band gap excitation at 2.2 eV arises from d−d transitions that are spin-allowed due to magnetic coupling between Fe atoms.[17] However, the interpretation of the major visible-light absorption feature at 3.2 eV[19] depends strongly on the theoretical model used. This peak was first explained as a ligand-to-metal charge transfer (LMCT) transition on the basis of self-consistent field Xα scattered wave[15] and semiempirical atom superposition and electron delocalization (ASED)[16] calculations. Later treatments[17] including a recent high-level

Received: September 16, 2013
Accepted: October 15, 2013
Published: October 15, 2013

   dx.doi.org/10.1021/jz401997d | J. Phys. Chem. Lett. 2013, 4, 3667−3671

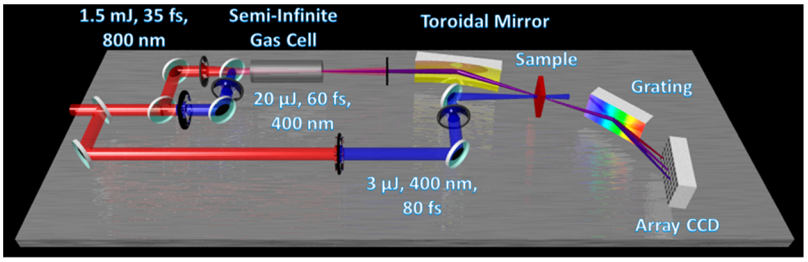

Figure 1. Diagram of the XUV transient absorption instrument. High harmonics are generated in a semi-infinite gas cell with a two-color driving field (1.5 mJ, 35 fs at 800 nm + 20 μJ, 60 fs at 400 nm). Residual 800/400 nm light is blocked with a total of 1.2 μm Al filters. The Ne pressure in the gas cell is 100 Torr (1.3×10^4 Pascals). The XUV beam is refocused onto the sample with a gold-coated toroidal mirror in grazing incidence, and the transmitted beam is diffracted from a concave variable line-spacing grating onto an array CCD. The sample is pumped at 400 nm with a 3 μJ, 80 fs pulse. Beyond the semi-infinite gas cell, the instrument is under vacuum ($\sim 10^{-6}$ Torr).

complete active space self-consistent field/complete active space with second-order perturbation theory (CASSCF/CASPT2) study[18] calculated this peak to be a d−d transition, with LMCT transitions (O^{2-} 2p → Fe^{3+} 3d) occurring at higher energy. The oxidation state and spin state specificity of $M_{2,3}$-edge absorption make it an excellent tool for distinguishing between these conflicting analyses.

The experimental apparatus is diagrammed in Figure 1. XUV transient absorption spectroscopy on a solid-state sample, in this case, a 14 nm thick α-Fe_2O_3 film on a 100 nm Si_3N_4 substrate,[20] poses unique experimental challenges beyond those faced in gas-phase studies.[5,6] Thin samples and substrates are required due to the short penetration depth of the probe beam. The substrate itself absorbs 90% of the XUV photons; therefore, the flux measured at the CCD detector is 10 times lower than that in a gas-phase experiment with the same sample absorbance. HHG is therefore performed in a semi-infinite gas cell[21] to maximize photon flux, stability, and ease of alignment. In order to improve the spectral coverage and minimize the low-flux regions between odd harmonics, a two-color laser field (800 nm + 400 nm)[22] is used to drive the HHG process. This breaks the inversion symmetry of the electric field and allows both even and odd harmonics to be produced. The average photon flux collected at the CCD from 47.5 to 67.5 eV is 2.6×10^4 photons/0.1 eV/sec (Figure 2A).

In addition to maximizing the XUV flux and stability, care is required to avoid sample damage from the pump beam. The 3 mm × 3 mm sample is raster-scanned between 2 s pump/probe data acquisitions, and approximately 2000 transient spectra are collected from one sample before there is a ∼10% reduction in the observed transient signal. Data from three identical samples are averaged to create the transient spectra, for a total data acquisition time of 3.5 h. The XUV continuum produced by HHG allows a full spectrum to be collected at once, as in an energy-dispersive beamline.[23] The spectrometer is calibrated using the first- and second-order absorption peaks of Xe gas. To minimize the effect of pump light scattering onto the CCD, difference spectra at time t are recorded in comparison to a spectrum taken at −500 fs. The chirp of the XUV probe pulse is not expected to be significant on the time scales presented here.[24]

The ground-state XUV absorption of the α-Fe_2O_3 film is shown in Figure 2B, with major and minor peaks at 57.5 and 53.7 eV, respectively. This spectrum is an excellent match for that of a hematite single crystal measured using a synchrotron source,[25] and electron diffraction was used to confirm the sample phase (see the Supporting Information). Static $M_{2,3}$-edge spectra of first-row transition metals have been discussed

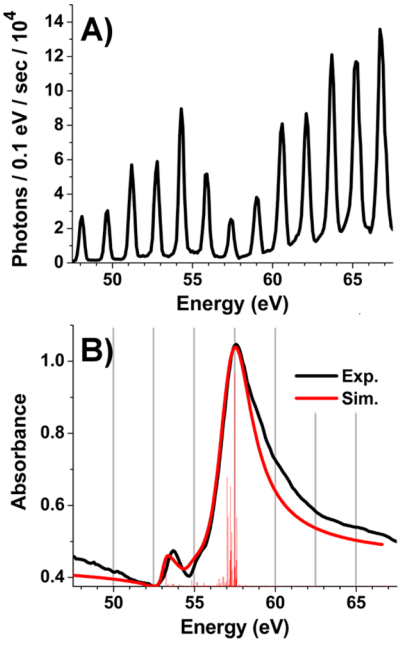

Figure 2. (A) Absolute XUV photon flux collected at the detector after passing through 14 nm thick α-Fe_2O_3 on 100 nm Si_3N_4. The use of odd and even harmonics produces excellent spectral coverage with sufficient flux for absorption spectroscopy, with an average of 2.6×10^4 photons/0.1 eV/sec from 47.5 to 67.5 eV. (B) Ground-state XUV absorption of a 14 nm thick α-Fe_2O_3 thin film. Black: experimental spectrum. Red line and sticks: ligand field multiplet simulation. See the Supporting Information for a discussion of the line broadening and Fano line shape.

in detail[26] and are calculated using a semiempirical ligand field multiplet model with the atomic charge, ligand field symmetry and strength, and a screening parameter as the only inputs.[3,25−27] Briefly, the Fe^{3+} cation in the octahedral ligand field of the surrounding O^{2-} anions has a ground-state electronic configuration of $^6A_1$ (Figure 3). In the absence of spin−orbit coupling, only two 3p → 3d transitions are allowed by spin and dipole selection rules, leading to the two observed absorption features. Unlike the 2p → 3d transition in $L_{2,3}$-edge absorption, spin−orbit coupling effects at the $M_{2,3}$-edge are weak and effectively only broaden the two peaks. The simulated spectrum shown in Figure 2B, calculated using the program CTM4XAS55[27] with the ligand field parameters of Berlasso et al.,[25] is an excellent match to the experimental spectrum. The absolute peak position determined from this calculation is approximate, and the energy axis is therefore shifted by −1.7 eV

dx.doi.org/10.1021/jz401997d | J. Phys. Chem. Lett. 2013, 4, 3667−3671

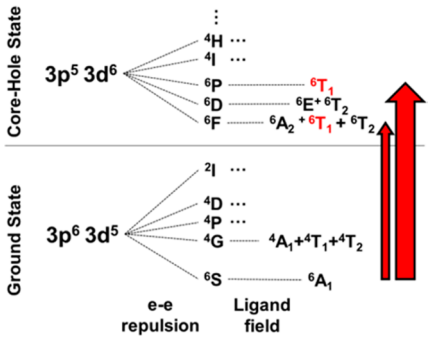

Figure 3. Diagram of initial and final states in the $M_{2,3}$-edge (3p → 3d) absorption of octahedral Fe^{3+}. Electron−electron repulsion splits the $3p^63d^5$ ground state and $3p^53d^6$ core−hole excited state into the atomic multielectron states ^6S, ^4G, and so forth, which are further split by the ligand field. In an octahedral field, the absorption of a photon transforms as the symmetry operation $^1T_1$, resulting in two spin- and dipole-allowed transitions. Spin−orbit coupling further splits and mixes the states (not shown in this diagram), effectively broadening these two transitions to produce the spectrum shown in Figure 2B.

to match the major peak position at 57.5 eV. The calculated stick spectrum is broadened, as described in the Supporting Information. All simulated spectra in this work use identical energy-axis shifting and broadening. In Figure 2A, the vertical axis of the simulated spectrum is shifted and scaled to best match the experimental result and account for a baseline of nonresonant absorption.

Photoexcitation of the α-Fe_2O_3 film with 3 μJ, 400 nm, 80 fs pulses causes a change in the shape of the $M_{2,3}$-edge spectrum indicative of the excited-state electronic structure (Figure 4A). Immediately after photoexcitation, the transient spectrum is characterized by a negative feature at 57.5 eV caused by depopulation of the ground state and three excited-state peaks at 52.9, 54.6, and 55.8 eV. Over the next 1 ps, the 55.8 eV peak increases and blue shifts, while the negative feature at 57.5 eV decays to ∼25% of its initial magnitude. No further spectral evolution is observed for delay times as long as 100 ps. Given the pump power of 3 μJ, spot size of 150 μm fwhm, and optical density at 400 nm of 0.5, it is estimated that one pump photon is absorbed per 20 Fe atoms. No significant change was seen in the spectra or kinetics at 1 μJ/pulse. Kinetic traces at absorption energies of 54.6, 56.4, and 57.4 eV are shown in Figure 4B. Because of the spectral overlap of the transient features, a global fit is performed on the full 2-D data set using the program GLOTARAN.[28] An excellent match to the experimental data is obtained by using a two-state sequential model ($A \xrightarrow{k} B$) with a time constant ($1/k$) of 240 ± 30 fs, convoluted with an 88 ± 3 fs Gaussian instrument response function (IRF). Errors are the standard deviation of the mean from four data sets on fresh samples. The two evolution-associated spectral components[29] identified by the fit are shown in Figure 4C, with the time evolution of each component shown in the inset.

The electronic structure of the short-lived initial photoexcited state is determined by comparing the experimental initial excited-state spectrum with simulated spectra of the possible LMCT and d−d excited states. Figure 5A shows simulated XUV absorption spectra of the $^5T_2$ Fe^{2+} state that would be formed from a LMCT transition and the $^4T_1$ Fe^{3+} state that would be formed from a d−d transition, calculated using the ligand field multiplet method described above. For consistency, all of the input parameters to the simulation except for the oxidation and spin state are identical to those used for the $^6A_1$ Fe^{3+} ground state in Figure 2B. The simulated spectrum of the LMCT state is red-shifted from that of the ground state, with two large peaks at 56.2 and 54.6 eV and a small peak at 52.2 eV. Core-level spectra of reduced species (Fe^{2+}) are red-shifted from their oxidized counterparts (Fe^{3+}), and the ∼2.5 eV shift is consistent with that observed in an electron energy-loss spectroscopy (EELS) study of the $Fe^{2+/3+}$ $M_{2,3}$-edge of a series of iron-containing minerals.[30] A red shift in Fe absorption upon photoreduction was also observed via picosecond time-resolved X-ray absorption spectroscopy at the Fe K-edge of dye-sensitized γ-Fe_2O_3 nanoparticles.[31]

The XUV absorption spectrum of the lowest-energy Fe^{3+} d−d excited state ($^4T_1$) is calculated to have a minor peak at 53.0 eV and major peaks at 58.8 and 63.8 eV (Figure 5A). Higher-energy d−d excited states such as $^4T_2$ are calculated to have spectra similar to that of the $^4T_1$ state, with a prominent absorption feature at around 64 eV. This net blue shift upon crossover from high to low/intermediate spin has been predicted for a range of 3d transition metals,[26] and a similar effect has been observed in the L_3-edge spectrum of the spin-crossover compound $[Fe(tren(py)_3)]^{2}$.[32] Note that these simulations do not take into account possible structural distortions resulting from the excitation.

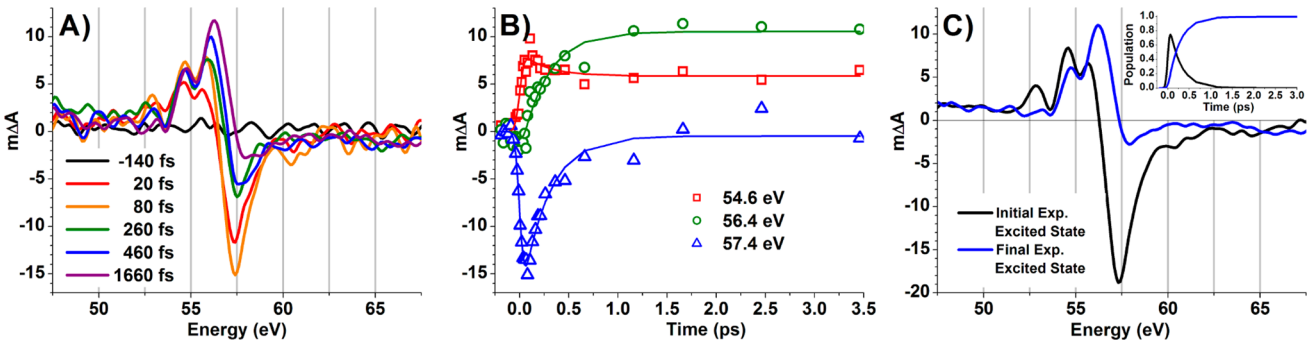

Figure 4. (A) XUV transient absorption spectra of α-Fe_2O_3 after excitation at 400 nm. Spectra are binned by 0.1 eV and smoothed using a 0.5 eV running boxcar average. (B) Kinetic traces at 54.6, 56.4, and 57.4 eV. Points are experimental data, and solid lines are from the global fit. (C) Evolution-associated spectra of the initial and final excited states obtained from a global fit using a two-state sequential ($A \xrightarrow{k} B$) model, convoluted with a Gaussian IRF. (Inset) Population of each state versus time. The fit identifies a time constant ($1/k$) of 240 ± 30 fs and an IRF of 88 ± 3 fs.

dx.doi.org/10.1021/jz401997d | J. Phys. Chem. Lett. 2013, 4, 3667−3671

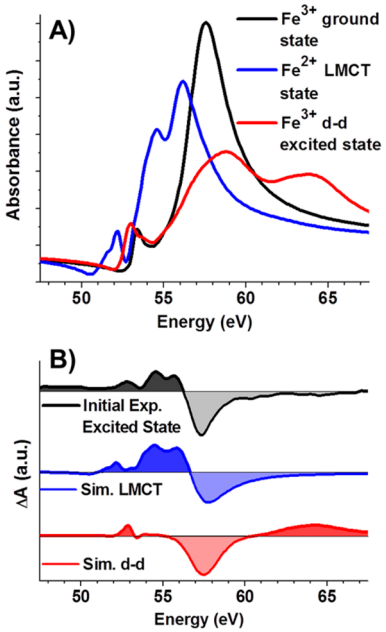

Figure 5. (A) Simulated XUV absorption spectra of the Fe^{3+} $^6A_1$ ground state, the Fe^{2+} $^5T_2$ state that would result from a LMCT excitation, and the Fe^{3+} $^4T_1$ state that would result from a d–d excitation. (B) Simulated difference spectra (excited state − ground state) compared to the experimental initial excited-state difference spectrum determined by the global fit. The experimental initial excited state is an excellent match for the simulated LMCT state, while the d–d excited state is predicted to show a large blue-shifted positive feature that is absent in the experimental spectrum.

Simulated difference spectra (excited state − ground state) of the LMCT and d–d excited states are shown in Figure 5B, along with the experimental difference spectrum of the initial excited state determined by the global fit. The simulated LMCT difference spectrum is an excellent match to the experimental difference spectrum, with similar shape and peak-to-peak spacing. On the other hand, the shape of the simulated d–d difference spectrum is qualitatively very different from that of the observed spectrum, most notably in the positive feature from 60 to 70 eV that is absent in the experiment.

The 240 fs time constant for conversion of the initial LMCT state to the final trap state is consistent with a reported ∼300 fs (instrument-response-limited) decay to a long-lived state observed with visible-light transient absorption spectroscopy of α-Fe_2O_3 nanoparticles[33] and thin films[34] after 400 nm excitation. This fast decay was assigned as hot electron relaxation, band filling, and/or band gap shrinkage. The long-lived state was attributed to trapping at either Fe^{3+} oxygen-deficient defects or midgap d–d states. Excess electrons on Fe atoms in α-Fe_2O_3 are thought to be stabilized by relaxation of the surrounding O atoms to form a small polaron, which has been observed with time-resolved Fe K-edge spectroscopy.[35] Such a polaron induced by the LMCT transition is therefore another possible identity of the long-lived state, as is trapping at the film surface or at grain boundary defects. Such states cannot be simulated using the semiempirical ligand field multiplet approach discussed above, which assumes a ligand field with well-defined symmetry. The long-lived trap state spectrum (Figure 4C) does not match that predicted for a d–d excited state (Figure 5B), suggesting that there is not a simple cascade to a low-lying d–d state and that geometric distortions may contribute to the final electronic state. Ab initio simulations[36−39] of the XUV spectra of possible trap states are ongoing and will be the subject of a future publication.

In conclusion, we have demonstrated the power of high-harmonic $M_{2,3}$-edge transient absorption spectroscopy to measure ultrafast photoinduced oxidation state changes in solid-state transition-metal systems. The strong oscillator strengths of the 3p → 3d transitions, electronic-state-specific peak shapes, and ultrafast time resolution make this an attractive alternative to synchrotron- and free-electron laser-based sources. Charge-transfer processes are central to photovoltaic and photocatalytic materials, and the ability to observe the flow of electrons in real time using a tabletop source will open up new possibilities in inorganic chemistry and materials science.

■ ASSOCIATED CONTENT

Supporting Information

Details of film fabrication and characterization by electron diffraction, UV–vis spectrum of the α-Fe_2O_3 film, and description of the line width of simulated spectra. This material is available free of charge via the Internet at http://pubs.acs.org.

■ AUTHOR INFORMATION

Corresponding Author

*E-mail: srl@berkeley.edu.

Present Address

◆J.V.-W.: Department of Chemistry, University of Illinois at Urbana/Champaign, Urbana, IL 61820.

Notes

The authors declare no competing financial interest.

■ ACKNOWLEDGMENTS

J.V.-W. and S.R.L. acknowledge support from The Office of Assistant Secretary of Defense for Research and Engineering, NSSEFF. Initial work by J.V.-W. was supported by the NSF ACC-F Postdoctoral Fellowship. Initial work by C.-M.J. was supported by the NSF Extreme Ultraviolet Engineering Resource Center for Extreme Ultraviolet Research and Technology (EEC-0310717). A.P.A., C.L., C.-M.J., H.G., P.Y., and instrument construction were supported by the Materials Science Division of Lawrence Berkeley National Laboratory by the U.S. Department of Energy at Lawrence Berkeley National Lab under Contract No. DE-AC02-05CH11231, "Physical Chemistry of Nanomaterials". J.M.L. is supported as part of the Light–Material Interactions in Energy Conversion, an Energy Frontier Research Center funded by the U.S. Department of Energy, Office of Science, Office of Basic Energy Sciences, under Contract DE-SC0001293. Daniel J. Hellebusch is thanked for analysis of TEM data.

■ REFERENCES

(1) Bressler, C.; Chergui, M. Molecular Structural Dynamics Probed by Ultrafast X-ray Absorption Spectroscopy. *Annu. Rev. Phys. Chem.* **2010**, *61*, 263–282.

(2) Chen, L. X. Probing Transient Molecular Structures in Photochemical Processes Using Laser-Initiated Time-Resolved X-ray Absorption Spectroscopy. *Annu. Rev. Phys. Chem.* **2005**, *56*, 221–254.

(3) de Groot, F. M. F.; Kotani, A. *Core Level Spectroscopy of Solids*; CRC Press: Boca Raton, FL, 2008.

(4) Corkum, P. B. Plasma Perspective on Strong-Field Multiphoton Ionization. *Phys. Rev. Lett.* **1993**, *71*, 1994–1997.

(5) Loh, Z. H.; Leone, S. R. Ultrafast Strong-Field Dissociative Ionization Dynamics of CH_2Br_2 Probed by Femtosecond Soft X-ray Transient Absorption Spectroscopy. *J. Chem. Phys.* **2008**, *128*, 204302.
(6) Loh, Z. H.; Khalil, M.; Correa, R. E.; Leone, S. R. A Tabletop Femtosecond Time-Resolved Soft X-ray Transient Absorption Spectrometer. *Rev. Sci. Instrum.* **2008**, *79*, 073101.
(7) Schultze, M.; Bothschafter, E. M.; Sommer, A.; Holzner, S.; Schweinberger, W.; Fiess, M.; Hofstetter, M.; Kienberger, R.; Apalkov, V.; Yakovlev, V. S.; et al. Controlling Dielectrics with the Electric Field of Light. *Nature* **2013**, *493*, 75−78.
(8) Goulielmakis, E.; Loh, Z. H.; Wirth, A.; Santra, R.; Rohringer, N.; Yakovlev, V. S.; Zherebtsov, S.; Pfeifer, T.; Azzeer, A. M.; Kling, M. F.; et al. Real-Time Observation of Valence Electron Motion. *Nature* **2010**, *466*, 739−743.
(9) La-O-Vorakiat, C.; Siemens, M.; Murnane, M. M.; Kapteyn, H. C.; Mathias, S.; Aeschlimann, M.; Grychtol, P.; Adam, R.; Schneider, C. M.; Shaw, J. M.; et al. Ultrafast Demagnetization Dynamics at the M Edges of Magnetic Elements Observed Using a Tabletop High-Harmonic Soft X-ray Source. *Phys. Rev. Lett.* **2009**, *103*, 257402.
(10) Turgut, E.; La-O-Vorakiat, C.; Shaw, J. M.; Grychtol, P.; Nembach, H. T.; Rudolf, D.; Adam, R.; Aeschlimann, M.; Schneider, C. M.; Silva, T. J.; et al. Controlling the Competition between Optically Induced Ultrafast Spin−Flip Scattering and Spin Transport in Magnetic Multilayers. *Phys. Rev. Lett.* **2013**, *110*, 197201.
(11) Sivula, K.; Le Formal, F.; Gratzel, M. Solar Water Splitting: Progress Using Hematite (α-Fe_2O_3) Photoelectrodes. *ChemSusChem* **2011**, *4*, 432−449.
(12) Sandratskii, L. M.; Uhl, M.; Kubler, J. Band Theory for Electronic and Magnetic Properties of α-Fe_2O_3. *J. Phys.: Condens. Matter* **1996**, *8*, 983−989.
(13) Canepa, P.; Schofield, E.; Chadwick, A. V.; Alfredsson, M. Comparison of a Calculated and Measured XANES Spectrum of α-Fe_2O_3. *Phys. Chem. Chem. Phys.* **2011**, *13*, 12826−12834.
(14) Ma, Y.; Johnson, P. D.; Wassdahl, N.; Guo, J.; Skytt, P.; Nordgren, J.; Kevan, S. D.; Rubensson, J. E.; Boske, T.; Eberhardt, W. Electronic-Structures of α-Fe_2O_3 and Fe_3O_4 from O K-Edge Absorption and Emission-Spectroscopy. *Phys. Rev. B* **1993**, *48*, 2109−2111.
(15) Tossell, J. A.; Vaughan, D. J.; Johnson, K. H. Electronic-Structure of Rutile, Wustite, and Hematite from Molecular-Orbital Calculations. *Am. Mineral.* **1974**, *59*, 319−334.
(16) Debnath, N. C.; Anderson, A. B. Optical-Spectra of Ferrous and Ferric Oxides and the Passive Film — A Molecular-Orbital Study. *J. Electrochem. Soc.* **1982**, *129*, 2169−2174.
(17) Sherman, D. M.; Waite, T. D. Electronic-Spectra of Fe^{3+} Oxides and Oxide Hydroxides in the Near IR to Near UV. *Am. Mineral.* **1985**, *70*, 1262−1269.
(18) Liao, P. L.; Carter, E. A. Optical Excitations in Hematite (α-Fe_2O_3) via Embedded Cluster Models: A CASPT2 Study. *J. Phys. Chem. C* **2011**, *115*, 20795−20805.
(19) Marusak, L. A.; Messier, R.; White, W. B. Optical Absorption Spectrum of Hematite, α-Fe_2O_3 Near IR to UV. *J. Phys. Chem. Solids* **1980**, *41*, 981−984.
(20) Gao, H. W.; Liu, C.; Jeong, H. E.; Yang, P. D. Plasmon-Enhanced Photocatalytic Activity of Iron Oxide on Gold Nanopillars. *ACS Nano* **2012**, *6*, 234−240.
(21) Sutherland, J. R.; Christensen, E. L.; Powers, N. D.; Rhynard, S. E.; Painter, J. C.; Peatross, J. High Harmonic Generation in a Semi-Infinite Gas Cell. *Opt. Express* **2004**, *12*, 4430−4436.
(22) Kim, I. J.; Kim, H. T.; Kim, C. M.; Park, J. J.; Lee, Y. S.; Hong, K. H.; Nam, C. H. Efficient High-Order Harmonic Generation in a Two-Color Laser Field. *Appl. Phys. B: Lasers Opt.* **2004**, *78*, 859−861.
(23) Phizackerley, R. P.; Rek, Z. U.; Stephenson, G. B.; Conradson, S. D.; Hodgson, K. O.; Matsushita, T.; Oyanagi, H. An Energy-Dispersive Spectrometer for the Rapid Measurement of X-ray Absorption-Spectra Using Synchrotron Radiation. *J. Appl. Crystallogr.* **1983**, *16*, 220−232.
(24) Mairesse, Y.; de Bohan, A.; Frasinski, L. J.; Merdji, H.; Dinu, L. C.; Monchicourt, P.; Breger, P.; Kovacev, M.; Auguste, T.; Carre, B.; Muller, H. G.; Agostini, P.; Salieres, P. High-Harmonics Chirp and Optimization of Attosecond Pulse Trains. *Laser Phys.* **2005**, *15*, 863−870.
(25) Berlasso, R.; Dallera, C.; Borgatti, F.; Vozzi, C.; Sansone, G.; Stagira, S.; Nisoli, M.; Ghiringhelli, G.; Villoresi, P.; Poletto, L.; et al. High-Order Laser Harmonics and Synchrotron Study of Transition Metals $M_{2,3}$ Edges. *Phys. Rev. B* **2006**, *73*, 115101.
(26) van der Laan, G. $M_{2,3}$ Absorption-Spectroscopy of 3d Transition-Metal Compounds. *J. Phys.: Condens. Matter* **1991**, *3*, 7443−7454.
(27) Stavitski, E.; de Groot, F. M. F. The CTM4XAS Program for EELS and XAS Spectral Shape Analysis of Transition Metal L Edges. *Micron* **2010**, *41*, 687−694.
(28) Snellenburg, J. J.; Laptenok, S.; Seger, R.; Mullen, K. M.; Van Stokkum, I. H. M. Glotaran: A Java-Based Graphical User Interface for the R Package TIMP. *J. Stat. Software* **2012**, *49*, 1−22.
(29) van Stokkum, I. H. M.; Larsen, D. S.; van Grondelle, R. Global and Target Analysis of Time-Resolved Spectra. *Biochim. Biophys. Acta, Bioenerg.* **2004**, *1657*, 82−104.
(30) van Aken, P. A.; Styrsa, V. J.; Liebscher, B.; Woodland, A. B.; Redhammer, G. J. Microanalysis of $Fe^{3+}/\Sigma Fe$ in Oxide and Silicate Minerals by Investigation of Electron Energy-Loss Near-Edge Structures (ELNES) at the Fe $M_{2,3}$ Edge. *Phys. Chem. Miner.* **1999**, *26*, 584−590.
(31) Katz, J. E.; Gilbert, B.; Zhang, X. Y.; Attenkofer, K.; Falcone, R. W.; Waychunas, G. A. Observation of Transient Iron(II) Formation in Dye-Sensitized Iron Oxide Nanoparticles by Time-Resolved X-ray Spectroscopy. *J. Phys. Chem. Lett.* **2010**, *1*, 1372−1376.
(32) Huse, N.; Cho, H.; Hong, K.; Jamula, L.; de Groot, F. M. F.; Kim, T. K.; McCusker, J. K.; Schoenlein, R. W. Femtosecond Soft X-ray Spectroscopy of Solvated Transition-Metal Complexes: Deciphering the Interplay of Electronic and Structural Dynamics. *J. Phys. Chem. Lett.* **2011**, *2*, 880−884.
(33) Cherepy, N. J.; Liston, D. B.; Lovejoy, J. A.; Deng, H.; Zhang, J. Z. Ultrafast Studies of Photoexcited Electron Dynamics in γ- and α-Fe_2O_3 Semiconductor Nanoparticles. *J. Phys. Chem. B* **1998**, *102*, 770−776.
(34) Joly, A. G.; Williams, J. R.; Chambers, S. A.; Xiong, G.; Hess, W. P.; Laman, D. M. Carrier Dynamics in α-Fe_2O_3 (0001) Thin Films and Single Crystals Probed by Femtosecond Transient Absorption and Reflectivity. *J. Appl. Phys.* **2006**, *99*, 053521.
(35) Katz, J. E.; Zhang, X. Y.; Attenkofer, K.; Chapman, K. W.; Frandsen, C.; Zarzycki, P.; Rosso, K. M.; Falcone, R. W.; Waychunas, G. A.; Gilbert, B. Electron Small Polarons and Their Mobility in Iron (Oxyhydr)oxide Nanoparticles. *Science* **2012**, *337*, 1200−1203.
(36) Ikeno, H.; Mizoguchi, T.; Tanaka, I. Ab Initio Charge Transfer Multiplet Calculations on the $L_{2,3}$ XANES and ELNES of 3d Transition Metal Oxides. *Phys. Rev. B* **2011**, *83*, 155107.
(37) Josefsson, I.; Kunnus, K.; Schreck, S.; Fohlisch, A.; de Groot, F.; Wernet, P.; Odelius, M. Ab Initio Calculations of X-ray Spectra: Atomic Multiplet and Molecular Orbital Effects in a Multiconfigurational SCF Approach to the L-Edge Spectra of Transition Metal Complexes. *J. Phys. Chem. Lett.* **2012**, *3*, 3565−3570.
(38) Maganas, D.; Roemelt, M.; Havecker, M.; Trunschke, A.; Knop-Gericke, A.; Schlogl, R.; Neese, F. First Principles Calculations of the Structure and V L-Edge X-ray Absorption Spectra of V_2O_5 Using Local Pair Natural Orbital Coupled Cluster Theory and Spin−Orbit Coupled Configuration Interaction Approaches. *Phys. Chem. Chem. Phys.* **2013**, *15*, 7260−7276.
(39) Roemelt, M.; Maganas, D.; DeBeer, S.; Neese, F. A Combined DFT and Restricted Open-Shell Configuration Interaction Method Including Spin−Orbit Coupling: Application to Transition Metal L-Edge X-ray Absorption Spectroscopy. *J. Chem. Phys.* **2013**, *138*, 204101.